STRUCTURAL INVESTIGATION AND HIRSHFELD SURFACE ANALYSIS OF Cu(II) TRIETHANOLAMINE 4-NITROBENZOATE

Anastasia GOROBET,[a] Manuela E. CRISAN,[b] Paulina N. BOUROSH[a] and Lilia CROITOR[a*]

[a]Institute of Applied Physics, Academy str., 5 MD2028, Chisinau, Republic of Moldova
[b]"Coriolan Drăgulescu" Institute of Chemistry, 24 Mihai Viteazu Blvd., 300223, Timişoara, Roumania

The crystal structure of new Cu(II) coordination compound synthesized using the triethanolammonium 4-nitrobenzoate (HTEA)(4NB), namely bis(4-nitrobenzoato)-bis(μ-2-[bis(2-hydroxyethyl)amino]ethan-1-olato)-di-copper(II) dihydrate $[Cu_2(TEA)_2(4NB)_2]\cdot2H_2O$, is reported. The compound consists of centrosymmetric dinuclear units, in which two Cu(II) ions are bridged by two $\mu:\eta_1$ oxo bridges of two TEA anions, adopting a NO_5 distorsional tetragonal bipyramidal geometry. Dinuclear complexes are hydrogen-bonded with outer-sphere water molecules by intermolecular O–H⋯O hydrogen bond interactions in a 1D supramolecular chain and further interlinked by C–H⋯π stacking interactions. The relationship between noncovalent interactions derived from Hirshfeld surface analysis, two-dimensional fingerprint plots and crystal lattice energy of the compound is also presented and discussed.
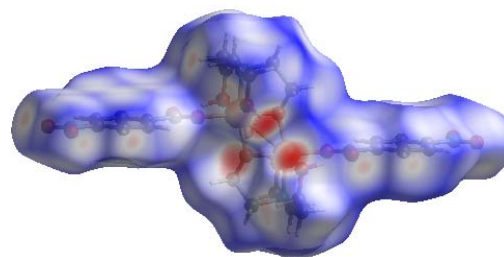
INTRODUCTION

Over the time, dinuclear Cu(II) amino alcohol complexes have received particular attention, as building blocks in metallo supramolecular chemistry,[1] as model of copper enzymes[2] and precursors of molecular magnetic and catalytic materials.[3,4] Depending on amino alcohol denticity, as well as on the size and shape of anion, discrete dinuclear Cu(II) molecules or Cu(II) coordination polymers with diverse dimensionalities were obtained.[5-8] The distance between Cu centres was correlated to the length of the ligands; the large Cu⋯Cu distance affects especially the enzyme activity (*e.g.* catecholase),[3] while short Cu⋯Cu distance influences the magnetic properties.[4] Cu(II) triethanolamine (TEA) carboxylate complexes utilized as selective catalyst for alkanes oxydation[9] and ferro-/antiferromagnetic behaviour[4,10] have been reported recently. Previously, we have shown the building blocks role of alkanolammonium benzoates in generating 1D-3D supramolecular architectures[11,12] and metal complexes,[13,14] their thermal stability,[15] low toxicity,[16,17] luminescence,[18] anticorrosive properties[19] and plant growth regulating effect.[20,21]

This study investigates the role of triethanolammonium 4-nitrobenzoate (HTEA) (4NB) in the structure formation of new dialkoxo bridged Cu(II) complex $[Cu_2(TEA)_2(4NB)_2]\cdot2H_2O$ with potential biological activity. The synthesis, structural characterization by X-ray structure analysis on a single crystal and infrared vibrational spectroscopy, as well as Hirshfeld surface of new Cu(II) complex were reported.

* Corresponding author: croitor.lilia@gmail.com

RESULTS AND DISCUSSION

1. IR Spectroscopy

The infrared spectrum of title compound is dominated by the characteristic absorptions of (HTEA)(4NB) ligand, such as strong bands $\nu_{as}(COO)$ and $\nu_s(COO^-)$ at 1567 cm^{-1} and 1344 cm^{-1} respectively. These indicate the existence of O-H⋯O hydrogen bonding between C=O of carboxylate and –OH group of TEA. The difference in the positions of carboxylate stretching vibrations (Δ=223 cm^{-1}) suggests monodentate coordination mode of carboxylate group to Cu(II) through deprotonated C–O group. The presence of water molecule in uncoordinated state in Cu(II) complex is confirmed by a broad band observed at 3395 cm^{-1}. In addition, several bands of medium intensity in the range 3000-2800 cm^{-1} refer to –(C-H) and –(O-H) vibrations of –CH$_2$ and –OH groups in TEA cation. Furthermore, the weak –(NO$_2$) vibration at 1524 cm^{-1} suggests that –NO$_2$ group of 4NB anion was not involved in hydrogen bonding or coordination. The ligand coordination to metal centre is revealed by bands at 635-531 cm^{-1}, which are mainly attributed to Cu-N and Cu-O stretching vibrations.[22]

2. Crystal structure

Compound **1** crystallizes in *P*–1 (№ 2) triclinic space group (Table 1) and the crystal structure consists of centrosymmetric dinuclear [Cu$_2$(TEA)$_2$(4NB)$_2$] entities (Figure 1a) with the two copper(II) atoms held together through two μ:η_1 oxo bridges of two TEA anions.

Each Cu(II) cation adopts a NO$_5$-six-coordinated distorted tetragonal bipyramidal geometry; the four coordination points in the equatorial plane are taken by two oxygen and one nitrogen atoms of two TEA anions, and one oxygen atom of carboxylic group of 4NB anion, while the apical positions are occupied by two oxygen atoms, O(5) and O(7), which belong to the –OH groups of the one TEA anion (Table 2). The copper atoms are displaced by 0.096 Å from the basal planes toward the apical positions. TEA coordinates in [*N,O,O,O*] tetradentate mode to the metal center with formation of three pentametallocycles, while 4NB – in monodentate coordination mode *via* O(1) atom. The uncoordinated to the metal center carboxylic oxygen atom of 4NB is involved as acceptor in intramolecular O(5)–H⋯O(2) (d(H⋯O)=1.79Å, d(O⋯O)=2.594(3) Å, ∠(OHO)=168°) hydrogen bond with one coordinated to the metal center –OH group of TEA ligand, giving rise to a six-membered cycle. The Cu⋯Cu separation within the dinuclear core is 2.921 Å.

The outer-sphere water molecules are hydrogen-bonded with dinuclear complexes through three ethanol groups of TEA molecules, acting as donors (O(1W)–H⋯O(5)(-*x*+1, -*y*+1, -*z*+1) with d(H⋯O)=1.97Å, d(O⋯O)=2.804(3) Å, ∠(OHO)=171° and O(1W)–H⋯O(6)(*x*+1, *y*, *z*) with d(H⋯O)=2.11Å, d(O⋯O)=2.917(3) Å, ∠(OHO)=165°) and an acceptor of protons (O(7)–H⋯O(1W), d(H⋯O)=1.87Å, d(O⋯O)=2.686(3) Å, ∠(OHO)=172°). Thus the components form a 1D hydrogen-bonding chain (Figure 1b) with Cu⋯Cu distance between adjacent metal-complexes within the supramolecular chain is equal to 7.488 Å. The obtained hydrogen-bonded chains are further interlinked by C–H⋯π stacking interactions with H⋯centroid and C–H⋯centroid distances equal to 2.86 and 3.822 Å, respectively (Figure 1c).

3. Hirshfeld surface analysis and fingerprint plots. Calculation of crystal lattice energies

Hirshfeld surface (HS) analysis[23] and two-dimensional (2D) fingerprint plots[24] generated by *CrystalExplorer17*[25] were carried out in order to investigate the nature and quantitative contributions of intermolecular interactions in the crystal packing of coordination complex **1**. The total d$_{norm}$ surface (ranging from -0.6974 (red) to 1.2220 (blue) Å) has been shown in Figure 2a, in which the red points (spherical depression spots) correspond to prominent O–H⋯O interactions in crystal. Red–blue triangle regions (bow–tie patterns) in the HS under the shape index function (from -1.0 (red) to 1.0 (blue) Å) demonstrate the presence of stacking interactions in the crystal (Figure 2b). Globularity (0.666) and asphericity (0.330) values quantified by the measurement of HS show that structure deviates from spherical surface and symmetry, respectively.
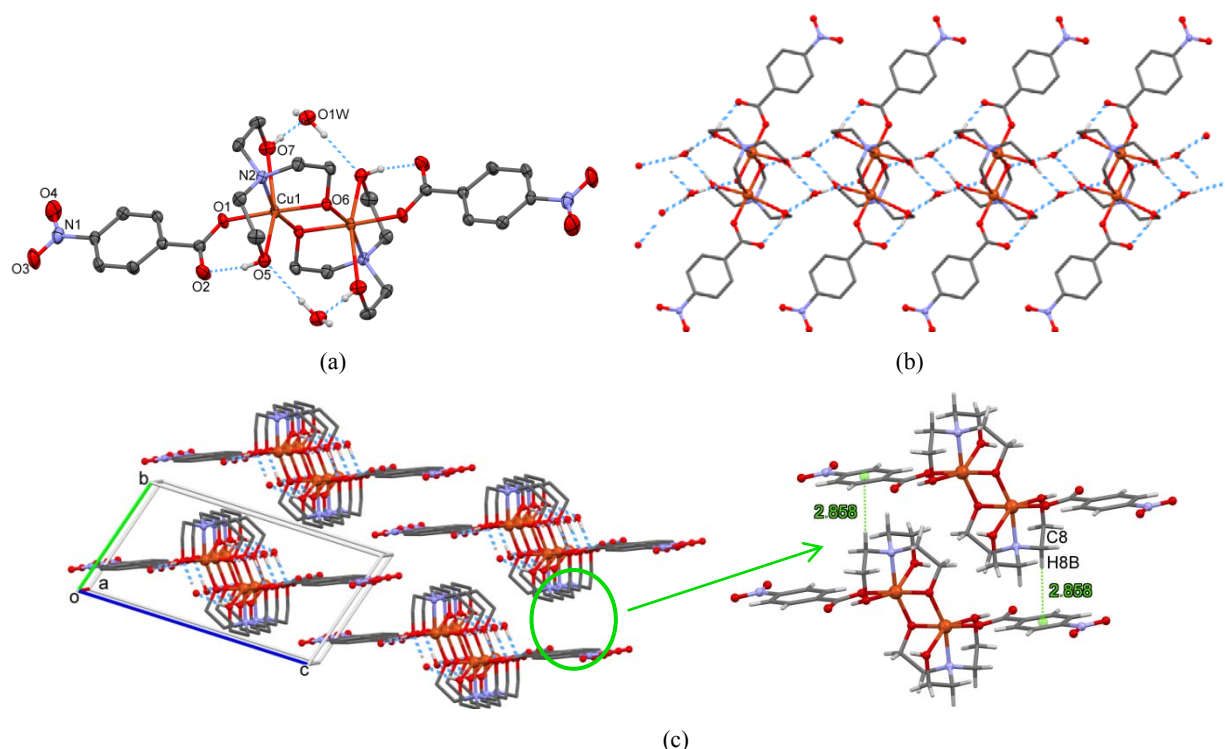
Fig. 1 – (a) The molecular structure of **1**, with partial atom-numbering scheme. Displacement ellipsoids are drawn at the 35% probability level. (b) Fragment of hydrogen-bonded supramolecular chain in **1**. C-bound H-atoms are omitted for clarity. (c) Fragment of crystal packing with the representation of C–H···π stacking interactions in detail. C-bound H atoms in crystal packing are omitted for clarity.

Table 1

Crystallographic data and structure refinement details for compound **1**

Crystal data			
Empirical formula	$C_{26}H_{40}Cu_2N_4O_{16}$	α(deg)	74.458(6)
Formula weight	791.70	β(deg)	86.428(7)
Temperature (K)	293(2)	γ(deg)	68.895(7)
Wavelength (Å)	0.71073	V(Å^3)	798.42(11)
Crystal system	Triclinic	Z	1
Space group	*P*-1 (№ 2)	D_c (g/cm^{-3})	1.647
a(Å)	7.4881(7)	μ(mm^{-1})	1.413
b(Å)	8.1977(5)	F(000)	410
c(Å)	14.4815(10)	Crystal size (mm^3)	0.62 × 0.11 × 0.05

Data collection and Refinement			
Reflections collected/unique	4801/2800 [R(int) = 0.0255]	GOF on F^2	0.998
Reflections with [$I>2\sigma(I)$]	2403	R_1, wR_2 [$I>2\sigma(I)$]	0.0360, 0.0856
Data/restraints/ parameters	2800 / 3 / 227	R_1, wR_2 (all data)	0.0449, 0.0921

Table 2

Selected bond distances (Å) and angles (°) in metal coordination cores in **1**

Parameter	Value	Parameter	Value	Parameter	Value
Cu(1)-O(1)	1.966(2)	Cu(1)-O(6)	1.944(2)	Cu(1)-O(6)^a	1.942(2)
Cu(1)-O(5)	2.539(2)	Cu(1)-O(7)	2.448(2)	Cu(1)-N(2)	2.051(2)
O(1)-Cu(1)-O(5)	88.75(8)	O(5)-Cu(1)-O(6)	90.72(8)	O(6)-Cu(1)-N(2)	84.64(8)
O(1)-Cu(1)-O(6)	177.40(7)	O(5)-Cu(1)-O(7)	153.40(8)	O(6)-Cu(1)-O(6)^a	82.56(8)
O(1)-Cu(1)-O(7)	85.32(9)	O(5)-Cu(1)-N(2)	78.81(8)	O(7)-Cu(1)-N(2)	76.36(9)
O(1)-Cu(1)-N(2)	97.75(8)	O(5)-Cu(1)-O(6)^a	113.84(8)	O(7)-Cu(1)-O(6)^a	92.54(8)
O(1)-Cu(1)-O(6)^a	95.32(8)	O(6)-Cu(1)-O(7)	96.27(8)	N(2)-Cu(1)-O(6)^a	162.04(9)

Symmetry transformations used to generate equivalent atoms: ^{a} -x+1, -y+1, -z+1
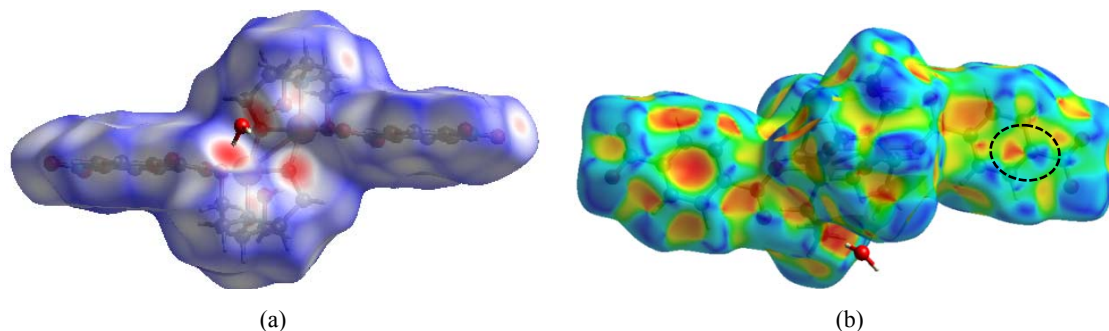
Fig. 2 – Hirshfeld surface for compound **1** plotted over d_{norm} *(a)* and shape index *(b)*.
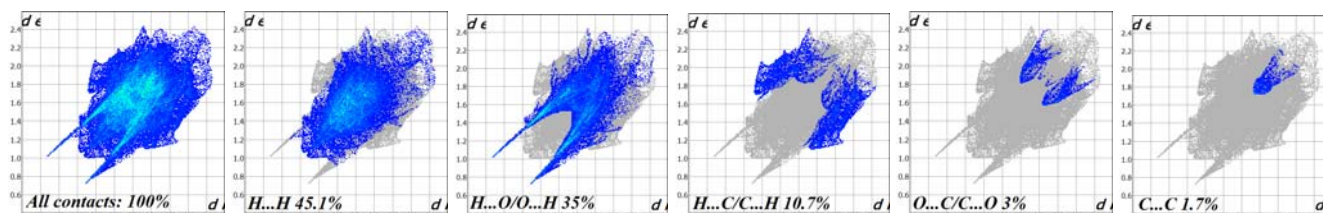
Fig. 3 – 2D fingerprint plots of **1** calculated from the Hirshfeld analysis.

The quantitative relationships between HS descriptors, as well as the nature and strength of bonding in crystals have been given by two-dimensional fingerprint plots, which clearly indicate the different distribution of interactions present in the crystal structure. 2D fingerprint plots are revealed by using the translated view with the d_i and d_e scales exposed on the graph axes (ranging from 0.67 to 2.48 Å). Decomposition of the full fingerprint plot for compound **1** shows nine principal types of interactions that include H⋯H, O⋯H/H⋯O, H⋯C/C⋯H, O⋯C/C⋯O, O⋯O, C⋯C, C⋯N/N⋯C, H⋯N/N⋯H and O⋯N/N⋯O contacts, in decreasing order (Figure 3). The major contribution to the total HS is made by H⋯H interactions, which appear in the middle of the scattered points in the fingerprint maps, and is about 45.1%. The next important interaction is O⋯H/H⋯O with a share of 35%, and with a significantly lower contribution – the H⋯C/C⋯H contacts, which usually represent C–H⋯π interactions, comprise 10.7% of the entire surface and are observed as two partly wide wing-like spikes in the 2D fingerprint plot. These data are in agreement with those observed in the structure and described above. The remaining HS is due to non-directional interactions such as O⋯C/C⋯O, O⋯O, C⋯C, C⋯N/N⋯C, H⋯N/N⋯H and O⋯N/N⋯O interactions, which contribute from 3% to 0.5%. The C⋯C contacts form 1.5% of all contacts, which correspond to π⋯π interactions. These contacts can be observed in the 2D fingerprint plot (Figure 3) as a blue triangle region (bow–tie pattern) or as red and blue triangles on the shape-index surface (Figure 2b). Analysing inter- and intramolecular interactions in our compound, we observe 2 types of stacking interactions: π⋯π and CH⋯π. The centroid⋯centroid distance between phenyl rings indicates a weak offset stacking interaction (4.134 Å).

Thus, on the base of the HS analysis, we can confirm the significant role of O–H⋯O and C–H⋯π interactions in the crystal packing of **1**. Moreover, we calculate an estimated value of the total interaction energy for molecular cluster generated by a pair of dimer molecules of **1**, joined together by C–H⋯π stacking interactions. The energy framework calculation was performed by employing CE-B3LYP/6-31G(d,p) energy model implemented in the *CrystalExplorer* computer program package with scale factors to determine E_{tot}: k_ele=1.057, k_pol=0.740, k_disp=0.871 and k_rep=0.618. The calculated interaction energies for electrostatic, dispersion, polarization, and repulsion are -9.9 kJ/mol, -5.2 kJ/mol, -60.3 kJ/mol, and 33.1 kJ/mol, respectively. The total energy is -46.4 kJ/mol. Thus, we can conclude that the dispersion interaction energy dominates over the electrostatic Coulomb interaction energy.

EXPERIMENTAL

The reagents (Cu(CH₃COO)₂·H₂O and TEA) were purchased from commercial sources and were used without further purification. The organic salt (HTEA)(4NB) was

prepared as described earlier in literature.[13] The IR spectrum was obtained in vaseline oil on a FTIR Spectrum-100 Perkin Elmer spectrometer in the range of 400 - 4000 cm^{-1}.

Synthesis and crystallization of [Cu$_2$(TEA)$_2$(4NB)$_2$]·2H$_2$O (1): Cu(CH$_3$COO)$_2$·H$_2$O (29.95 mg, 0.15 mmol) and (HTEA)(4NB) (47.45 mg, 0.15 mmol) were dissolved in H$_2$O (6 mL), in which 3 drops (0.12 mL) TEA were added and the reaction mixture was stirred under air condition, at 45°C for ~ 15 min. The resulted blue-transparent solution was filtered off and then slowly cooled to room temperature. Plate blue crystals were precipitated after two months. Yield: 74%.

Refinement: Single crystal X-ray diffraction measurement for **1** was carried out on a Xcalibur E CCD diffractometer equipped with a CCD area detector and a graphite monochromator utilizing MoKα radiation at room temperature. All H atoms bonded to C atoms were refined using a riding-model approximation, with C–H = 0.93 and 0.97 Å for CH (aromatic) and CH$_2$ groups, respectively, which were fixed with U$_{iso}$(H) = 1.2U$_{eq}$(C). O-bound H atoms were positioned geometrically and treated as riding atoms using SHELXL default parameters (AFIX 147 instruction, in SHELXL2014[26]) with U$_{iso}$(H) = 1.5Ueq(C). Hydrogen atoms attached to O-atoms in water molecule were found from differential Fourier maps at the intermediate stages of the refinement and their positions were restrained using DFIX instructions for O–H (0.90 Å) and H···H (1.46 Å) distances. The Figures were produced using the Mercury program[27]. Crystallographic data of the new structure reported herein were deposited with the Cambridge Crystallographic Data Centre and allocated the deposition number CCDC 2047770.

Theoretical calculations: The Hirshfeld surface analysis was carried out using *CrystalExplorer* 17.5[25] program to quantify and visualize different molecular interactions. The interaction energies between the two molecules which form a cluster were calculated from the monomer wave functions at B3LYP/6-31G(d,p) for the 3D energy framework analysis.

CONCLUSIONS

The investigation of the crystal structure of a new Cu(II) triethanolamine 4-nitrobenzoate indicates that noncovalent intermolecular interactions, such as O–H···O and C–H···π, contribute to the components packing in the crystal. The Hirshfeld surface and the 2D fingerprint plots have been used to quantify these interactions and to show their priority.

REFERENCES

1. M. Andruh, *Chem. Commun.*, **2007**, *25*, 2565–2577.
2. R. H. Holm, P. Kennepohl and E. I. Solomon, *Chem. Rev.* **1996**, *96*, 2239–2314.
3. P. Zerón, M. Westphal, P. Comba, M. Flores-Álamo, A. C. Stueckl, C. Leal-Cervantes, V. M. Ugalde-Saldívar and L. Gasque, *Eur. J. Inorg. Chem.*, **2017**, 56–62.
4. R. P. Sharma, A. Saini, D. Monga, P. Venugopalan, J. Jezierska, A. Ozarowskic and V. Ferretti, *New J. Chem.*, **2014**, *38*, 437–447.
5. A. M. Kirillov, M. Haukka, M. N. Kopylovich and A. J. L. Pombeiro, *Acta Crystallogr. E*, **2007**, *63* m526-m528.
6. Z. Boulsourani, G. D. Geromichalos, K. Repana, E. Yiannaki, V. Psycharis, C. P. Raptopoulou, D. Hadjipavlou-Litina, E. Pontiki and C. Dendrinou-Samara, *J. Inorg. Biochem.*, **2011**, *105*, 839–849.
7. M. Andruh, *Pure Appl. Chem.*, **2005**, *77*, 1685–1706.
8. C. R. Groom, I. J. Bruno, M. P. Lightfoot and S. C. Ward, *Acta Cryst.*, **2016**, B72, 171–179.
9. P. Seppälä, R. Sillanpää and A. Lehtonen, *Coord. Chem. Rev*, **2017**, *347*, 98–114.
10. R. P. Sharma, A. Saini, P. Venugopalan, V. Ferretti, F. Spizzo, C. Angeli and C. J. Calzado, *New J. Chem.,* **2014**, *38*, 574–583.
11. Y. M. Chumakov, Y. A. Smirnov, M. Grozav, M. Crisan, G. Bocelli, A. A. Yakovenko and D. Lyubetsky, *Cent. Eur. J. Chem.*, **2006**, *4*, 458–475.
12. L. Croitor, M. F. Petric, E. I. Szerb, G. Vlase, P. Bourosh, Y. Chumakov and M. E. Crisan, *CrystEngComm*, **2019**, *21*, 6038–6047.
13. A. Gorobet, M. E. Crisan, P. Bourosh, A. Siminel and L. Croitor, *Polyhedron,* **2021**, *193*, 114893.
14. A. Gorobet, M. Crisan, M. Petric, P. Bourosh and L. Croitor, *Rev. Roum. Chim.*, **2018**, *63*, 1175–1179.
15. M. Crisan, G. Vlase, E. I. Szerb and T. Vlase, *J. Therm. Anal. Calorim.*, **2018**, *132*, 1409–1418.
16. S. A. Chicu, M. Grozav, L. Kurunczi and M. Crisan, *Rev. Chim. (Bucharest)*, **2008**, *59*, 582–587.
17. M. Crisan, L. Halip, P. Bourosh, S. A. Chicu and Y. Chumakov, *Chem. Cent. J.*, **2017**, *11*, 129–139.
18. L. Croitor, M. Petric, G. Vlase, T. Vlase, A. V. Siminel, P. Bourosh and M. Crisan, *J. Therm. Anal. Calorim.*, **2020**, *141*, 973–979.
19. M. Crisan, G. Vlase, N. Plesu, M. Petric, L. Croitor, V. Kravtsov, Y. Chumakov, P. Bouros and T. Vlase, *J. Therm. Anal. Calorim.*, **2018**, *134*, 343–352.
20. L. Croitor, M. Crisan, G. Vlase, T. Vlase, F. Bodnarescu, R. Sumalan, M. Petric, A. V. Siminel and P. Bourosh, *J. Therm. Anal. Calorim.*, **2020**, *142*, 191–201.
21. R. L. Sumalan, L. Croitor, M. Petric, I. Radulov, P. Bourosh, R. M. Sumalan and M. Crisan, *Molecules*, **2020**, *25*, 1635–1649.
22. K. Nakamoto, "Infrared spectra of inorganic and coordination compounds", 5th edition, John Wiley, New York, 1997.
23. F. L. Hirshfeld, *Theor. Chim. Acta,* **1977,** *44,* 129–138.
24. M. A. Spackman and D. Jayatilaka, *CrystEngComm*, **2009**, *11*, 19–32.
25. S. K. Wolff, D. J. Grimwood, J. J. McKinnon, M. J. Turner, D. Jayatilaka and M. A. Spackman, **2012**, *CrystalExplorer*, University of Western Australia, Australia.
26. G. M. Sheldrick, *Acta Cryst. ,* **2015**, *C71*, 3–8.
27. C. F. Macrae, P. R. Edgington, P. McCabe, E. Pidcock, G. P. Shields, R. Taylor, M. Towler and J. van de Streek, *J. Appl. Crystallogr.*, **2006**, *39*, 453–457.